A Hybrid Perturbative-Stochastic Galerkin Method for the Variability Analysis of Nonuniform Transmission Lines

A Hybrid Perturbative-Stochastic Galerkin Method for the Variability Analysis of Nonuniform Transmission Lines

Xinglong Wu, *Student Member, IEEE,* Paolo Manfredi, *Senior Member, IEEE,* Dries Vande Ginste, *Senior Member, IEEE,* Flavia Grassi, *Senior Member, IEEE.*

***Abstract*—In this paper, a hybridization of the classical stochastic Galerkin method (SGM) with two perturbative solution techniques is proposed to speed up the statistical analysis of nonuniform multiconductor transmission line (MTL) structures with parameters affected by uncertainty. The first method leverages a recently-developed deterministic perturbation technique (PT) to deal with nonuniformity affecting the SGM-augmented MTL equations. This approach is proven to be computationally more efficient than the traditional solution based on line subdivision into uniform cascaded sections, yet its performance is still affected by the so-called "curse of dimensionality". To further mitigate this issue, a second method is proposed, which resorts to the solution of uncoupled MTLs having the same size as the original structure, and where the effects of both nonuniformity and stochasticity are iteratively included by means of distributed sources. The accuracy and computational efficiency of the proposed approaches are assessed based on the statistical prediction of the mixed-mode S-parameters of microstrip-line structures with different numbers of random parameters. The test cases demonstrate that the hybrid SGM-PT approach is applicable to problems with a few tens of random variables, which is an unprecedented result for state-of-the-art SGM implementations.**

***Index Terms*—Nonuniform multiconductor transmission lines, perturbation technique, polynomial chaos, stochastic Galerkin method, uncertainty quantification.**

I. Introduction

MULTICONDUCTOR transmission lines (MTLs) are widely used in modern high-speed electronic systems. The variability of their geometrical or material parameters due to design constraints or manufacturing tolerances makes it difficult or even impossible to predict their performance deterministically [1]. Therefore, statistical analysis of MTL structures during the early design stage is a fundamental tool for the assessment of the circuit performance and for guiding the design and fabrication process.

One popular approach for stochastic analysis is the sampling-based Monte Carlo (MC) method. However, uncertainties such as trace widths and spacings, as well as material permittivity, require a large set of simulation samples, which hinders the application of MC to complex structures. This inefficiency is exacerbated when dealing with nonuniform MTLs, since the standard approach is to approximate such lines as a cascade of uniform sections [2], [3]. This is hereafter denoted as the uniform cascaded section (UCS) method, and it further increases the computational time of repeated-run analyses.

To alleviate this computational burden, it was recently proposed to analyze nonuniform MTLs by means of a perturbation technique (PT) [4]–[7]. The underlying idea is to interpret nonuniformity in MTLs as a perturbation of an average or ideal uniform line. The original MTL equations with place-dependent per-unit-length (p.u.l.) matrices are then suitably recast as the equations of a uniform line driven by equivalent distributed sources accounting for line nonuniformity. Furthermore, the corresponding circuit interpretation, providing physical insight in the mechanism of mode conversion in differential signaling, was described in [8], [9]. An application of this technique to a MC-based statistical analysis is found in [10].

Such a PT allows to substantially speed up a MC analysis, but it still does not solve the issue related to the huge amount of required samples. To overcome this limitation, several methods based on polynomial chaos expansion (PCE) theory [11] have been developed [12]–[17]. These methods approximate the uncertainty using expansions into orthogonal polynomials. Among them, the stochastic Galerkin method (SGM) was proven to be highly accurate compared to other non-intrusive approaches such as collocation methods [17]–[19]. In some cases, collocation methods can be rigorously proven to be an approximation of the SGM [19]. Rather than making use of repeated simulations, the SGM develops and solves a single, deterministic yet augmented problem. The accuracy and computational efficiency of the SGM in the analysis of MTLs have been thoroughly assessed and verified in literature. Nevertheless, because of its intrusive feature, SGM-based analyses rapidly suffer from the so-called "curse of dimensionality", and they can therefore account for small numbers of random variables (RVs) only.

In this work, a hybridization of the SGM with perturbative methods is proposed to expedite the variability analysis of nonuniform MTLs. In a first step, the PT is applied directly to the SGM problem pertaining to a nonuniform MTL. Unlike the classical UCS method, the new technique solves the augmented problem as a single uniform MTL section with

X. Wu and F. Grassi are with the Department of Electronics, Information and Bioengineering, Politecnico di Milano, Milan 20133, Italy (e-mail: xinglong.wu@polimi.it; flavia.grassi@polimi.it).

P. Manfredi is with the Department of Electronics and Telecommunications, Politecnico di Torino, Turin 10129, Italy (e-mail: paolo.manfredi@polito.it).

D. Vande Ginste is with the Department of Information Technology, IDLab/Electromagnetics Group, Ghent University-imec, Gent 9000, Belgium (e-mail: dries.vandeginste@ugent.be).

average p.u.l. matrices and equivalent distributed sources. As a further step, a *decoupled* perturbative SGM is introduced, which allows solving the various perturbation steps separately for each PCE coefficient. Owing to its decoupled structure, this novel method scales better with the number of unknown PCE coefficients, thus mitigating the curse of dimensionality. Unlike the state-of-the-art SGM, whose applications are limited to cases with small numbers of RVs, the proposed hybrid SGM-PT is applicable to problems with a few tens of RVs, which is an unprecedented result.

The paper is organized as follows. Section II reviews the PT for the analysis of nonuniform MTLs. Section III outlines the combination of the standard PT with the classical SGM for the stochastic analysis of nonuniform MTLs. In Section IV, the improved, decoupled perturbative SGM is presented. The computational efficiency of the proposed approaches is discussed in Section V. In Section VI, the proposed techniques are applied to the stochastic analysis of differential nonuniform MTLs, demonstrating their accuracy and computational efficiency. Finally, conclusions are drawn in Section VII.

II. Analysis of Nonuniform MTLs

The general frequency-domain equations for a nonuniform MTL with N signal conductors along z are defined as

$$\begin{cases} \dfrac{d}{dz}\boldsymbol{V}(z,\omega) = -j\omega\boldsymbol{L}(z,\omega)\boldsymbol{I}(z,\omega) \\ \dfrac{d}{dz}\boldsymbol{I}(z,\omega) = -j\omega\boldsymbol{C}(z,\omega)\boldsymbol{V}(z,\omega) \end{cases} \tag{1}$$

where $\omega = 2\pi f$ is the angular frequency, vectors $\boldsymbol{V}$ and $\boldsymbol{I}$ collect the line voltages and currents, and matrices $\boldsymbol{L}$ and $\boldsymbol{C}$ are the $N \times N$ *complex* p.u.l. inductance and capacitance matrices. These are defined as

$$\begin{cases} \boldsymbol{L}(z,\omega) = \mathsf{L}(z,\omega) + \mathsf{R}(z,\omega)/(j\omega) \\ \boldsymbol{C}(z,\omega) = \mathsf{C}(z,\omega) + \mathsf{G}(z,\omega)/(j\omega) \end{cases} \tag{2}$$

and encompass the classical (frequency- and position-dependent) p.u.l. resistance R, inductance L, conductance G, and capacitance C matrices. Hereafter, the argument ω is omitted for brevity of notation.

In order to solve (1), the UCS method approximates the nonuniform MTL as the cascade of uniform sections with constant p.u.l. matrices. The overall multiport representation for this modified structure is readily computed from the exponential stamp of each section [3], [20] and combined with proper terminal conditions to obtain the desired responses [2].

Alternatively, by using a perturbative approach [5], [7], [9], the p.u.l. matrices are expressed as a place-dependent perturbation of a constant reference matrix, i.e.,

$$\begin{cases} \boldsymbol{L}(z) = \bar{\boldsymbol{L}} + \Delta\boldsymbol{L}(z) \\ \boldsymbol{C}(z) = \bar{\boldsymbol{C}} + \Delta\boldsymbol{C}(z) \end{cases} \tag{3}$$

where the reference matrices $\bar{\boldsymbol{L}}$ and $\bar{\boldsymbol{C}}$ are taken as the average of the corresponding p.u.l. matrices along the z-axis. Replacing (3) into (1) yields the equation

$$\begin{cases} \dfrac{d}{dz}\boldsymbol{V}(z) = -j\omega\bar{\boldsymbol{L}}\boldsymbol{I}(z) - j\omega\Delta\boldsymbol{L}(z)\boldsymbol{I}(z) \\ \dfrac{d}{dz}\boldsymbol{I}(z) = -j\omega\bar{\boldsymbol{C}}\boldsymbol{V}(z) - j\omega\Delta\boldsymbol{C}(z)\boldsymbol{V}(z) \end{cases} \tag{4}$$

By assuming $\Delta\boldsymbol{L} \ll \bar{\boldsymbol{L}}$ and $\Delta\boldsymbol{C} \ll \bar{\boldsymbol{C}}$ (this condition is quantified in Section V), (4) is interpreted as a perturbation equation and solved iteratively as

$$\begin{cases} \dfrac{d}{dz}\boldsymbol{V}_m(z) = -j\omega\bar{\boldsymbol{L}}\boldsymbol{I}_m(z) + \boldsymbol{V}_{F,m}(z) \\ \dfrac{d}{dz}\boldsymbol{I}_m(z) = -j\omega\bar{\boldsymbol{C}}\boldsymbol{V}_m(z) + \boldsymbol{I}_{F,m}(z) \end{cases} \tag{5}$$

where

$$\begin{cases} \boldsymbol{V}_{F,m}(z) = -j\omega\Delta\boldsymbol{L}(z)\boldsymbol{I}_{m-1}(z) \\ \boldsymbol{I}_{F,m}(z) = -j\omega\Delta\boldsymbol{C}(z)\boldsymbol{V}_{m-1}(z) \end{cases} \tag{6}$$

and the subscript "m" denotes the iteration step, with $m > 0$. It should be noted that (5) corresponds to the equation for a *uniform* MTL with distributed sources, similarly to the case of an MTL excited by an external impinging electromagnetic wave [3], [7]. The distributed sources here depend on the available solution at the previous iteration step, and add to the original lumped excitation at the terminations. The "zero-order" contributions for $m = 0$ (i.e., $\boldsymbol{V}_0$ and $\boldsymbol{I}_0$) are obtained as the solution of the average uniform MTL, i.e. (5) with $\boldsymbol{V}_{F,0} = 0$ and $\boldsymbol{I}_{F,0} = 0$. The actual value of the line voltages and currents is then obtained as the limit for increasing iterations, i.e.,

$$\begin{cases} \boldsymbol{V}(z) &= \lim\limits_{m\to\infty} \boldsymbol{V}_m(z) \\ \boldsymbol{I}(z) &= \lim\limits_{m\to\infty} \boldsymbol{I}_m(z) \end{cases} \tag{7}$$

The distributed sources are updated at each iteration step, and the process is terminated when the solution has converged within a predefined threshold (set to a relative difference of 0.1% in this work).

III. Variability Analysis of Nonuniform MTLs

Assume the MTL (1) be affected by d random parameters described by vector $\boldsymbol{\xi} = [\xi_1, \ldots, \xi_d]$, which makes the p.u.l. matrices dependent on $\boldsymbol{\xi}$. In turn, the line voltages $\boldsymbol{V}$ and currents $\boldsymbol{I}$ also become stochastic. The classical MC approach amounts to repeatedly solving (1) for different realizations of the random parameters, thus generating a sufficiently large number of voltage/current samples to extract pertinent statistical information.

Alternatively, the SGM relies on representing the stochastic ($\boldsymbol{\xi}$-dependent) p.u.l. matrices by the following PCEs:

$$\begin{cases} \boldsymbol{L}(z,\boldsymbol{\xi}) = \sum\limits_{k=0}^{K-1} \boldsymbol{L}_k(z)\varphi_k(\boldsymbol{\xi}) \\ \boldsymbol{C}(z,\boldsymbol{\xi}) = \sum\limits_{k=0}^{K-1} \boldsymbol{C}_k(z)\varphi_k(\boldsymbol{\xi}) \end{cases} \tag{8}$$

where the functions $\{\varphi_k\}_{k=0}^{K-1}$ form a basis of multivariate orthogonal polynomials. For most probability distributions of $\boldsymbol{\xi}$, the optimal basis functions (yielding the best convergence rate) are readily available [11]. Without loss of generality, independent Gaussian distributions are considered in this paper, which implies that Hermite polynomials are used as basis functions. The approach is readily extended to other distribution types by properly changing the basis functions. In

particular, numerical techniques exist to calculate orthogonal polynomials for non-standard [21] and possibly correlated distributions [22].

The number of terms in each PCE (8) is related to the number of random parameters d by

$$K = \frac{(p+d)!}{p!d!} \tag{9}$$

where p is the maximum degree of the polynomials (for most applications, p lies in the range $[2, 4]$). The PCE coefficients in (8) are numerically determined based on the known stochastic variation of the MTL geometry and/or material properties [12], [23].

Next, similar PCE representations are assumed for the voltages and currents, i.e.,

$$\begin{cases} \boldsymbol{V}(z,\boldsymbol{\xi}) = \sum_{k=0}^{K-1} \boldsymbol{V}_k(z)\varphi_k(\boldsymbol{\xi}) \\ \boldsymbol{I}(z,\boldsymbol{\xi}) = \sum_{k=0}^{K-1} \boldsymbol{I}_k(z)\varphi_k(\boldsymbol{\xi}) \end{cases} \tag{10}$$

Substituting (8) and (10) into (1), and subsequently performing a Galerkin projection, leads to an augmented and *deterministic* system of coupled MTL-like equations in the unknown voltage and current PCE coefficients [17]:

$$\begin{cases} \frac{d}{dz}\widetilde{\mathbf{V}}(z) = -j\omega\widetilde{\mathbf{L}}(z)\widetilde{\mathbf{I}}(z) \\ \frac{d}{dz}\widetilde{\mathbf{I}}(z) = -j\omega\widetilde{\mathbf{C}}(z)\widetilde{\mathbf{V}}(z) \end{cases} \tag{11}$$

where $\widetilde{\mathbf{V}} = [\boldsymbol{V}_0, \ldots, \boldsymbol{V}_{K-1}]$ and $\widetilde{\mathbf{I}} = [\boldsymbol{I}_0, \ldots, \boldsymbol{I}_{K-1}]$, whereas the new p.u.l. matrices $\widetilde{\mathbf{L}}(z)$ and $\widetilde{\mathbf{C}}(z)$ are constructed block-wise using suitable weighed combinations of the PCE coefficients. For an original stochastic nonuniform MTL with N conductors, equation (11) is equivalent to a *deterministic* nonuniform MTL with NK conductors, whose voltages and currents are the PCE coefficients of the original quantities.

Hence, the resulting equations are formally equivalent to those of a nonuniform MTL (see (1)), and they can be solved by means of either the UCS method or the PT outlined in Section II. Owing to the size of the augmented MTL equation, the latter allows achieving a substantial speed-up, as will be shown in Section VI. It should be noted that the corresponding constant reference matrices, defined as in (3), are in this case *fully coupled*, thus dense, and have a potentially huge size of $NK \times NK$. Nevertheless, the PT avoids analyzing multiple sections of this size, but rather limits the solution to a single uniform section (5) with proper distributed sources (6).

Upon determination of the pertinent PCE coefficients, (10) are readily used as macromodels for a fast sampling of the stochastic voltages and currents, and extraction of statistical information such as the probability density functions (PDF). Moreover, following the general properties of PCEs [11], average and standard deviation are directly obtained from the PCE coefficients as:

$$\mathrm{E}\{\boldsymbol{V}(z,\boldsymbol{\xi})\} = \boldsymbol{V}_0(z) \tag{12a}$$

$$\sqrt{\mathrm{Var}\{\boldsymbol{V}(z,\boldsymbol{\xi})\}} = \sqrt{\sum_{k=1}^{K-1} |\boldsymbol{V}_k(z)|^2} \tag{12b}$$

IV. Decoupled Perturbative SGM

Despite the expected efficiency improvement, the method proposed in the previous section still needs to deal with fully coupled augmented MTL equations, which limits the computational efficiency for very large problems. In this section, a decoupled approach of the nonuniform SGM problem is introduced, allowing for a separate solution of each PCE coefficient.

The novel approach starts by noting that, since φ_0 is constant for any polynomial basis [11], the zero-order terms in the PCEs (8) are actually deterministic (i.e., $\boldsymbol{\xi}$-independent). Upon proper normalization of the basis, $\varphi_0 = 1$, and thus:

$$\begin{cases} \boldsymbol{L}(z,\boldsymbol{\xi}) = \boldsymbol{L}_0(z) + \sum_{k=1}^{K-1} \boldsymbol{L}_k(z)\varphi_k(\boldsymbol{\xi}) \\ \boldsymbol{C}(z,\boldsymbol{\xi}) = \boldsymbol{C}_0(z) + \sum_{k=1}^{K-1} \boldsymbol{C}_k(z)\varphi_k(\boldsymbol{\xi}) \end{cases} \tag{13}$$

Nonetheless, $\boldsymbol{L}_0$ and $\boldsymbol{C}_0$ are still z-dependent (i.e., nonuniform). Therefore, the next step is to express them as in (3), i.e.,

$$\begin{cases} \boldsymbol{L}_0(z) = \bar{\boldsymbol{L}}_0 + \Delta\boldsymbol{L}_0(z) \\ \boldsymbol{C}_0(z) = \bar{\boldsymbol{C}}_0 + \Delta\boldsymbol{C}_0(z) \end{cases} \tag{14}$$

By aggregating the place-dependent perturbations in (14) to the summations in the r.h.s. of (13), the p.u.l. matrices are eventually expressed as

$$\begin{cases} \boldsymbol{L}(z,\boldsymbol{\xi}) = \bar{\boldsymbol{L}}_0 + \Delta\boldsymbol{L}(z,\boldsymbol{\xi}) = \bar{\boldsymbol{L}}_0 + \sum_{k=0}^{K-1} \Delta\boldsymbol{L}_k(z)\varphi_k(\boldsymbol{\xi}) \\ \boldsymbol{C}(z,\boldsymbol{\xi}) = \bar{\boldsymbol{C}}_0 + \Delta\boldsymbol{C}(z,\boldsymbol{\xi}) = \bar{\boldsymbol{C}}_0 + \sum_{k=0}^{K-1} \Delta\boldsymbol{C}_k(z)\varphi_k(\boldsymbol{\xi}) \end{cases} \tag{15}$$

with $\Delta\boldsymbol{L}_k(z) \equiv \boldsymbol{L}_k(z)$ and $\Delta\boldsymbol{C}_k(z) \equiv \boldsymbol{C}_k(z)$ for $k > 0$, i.e., the sum of a deterministic, position-invariant term and a stochastic place-dependent perturbation. It should be noted that $\bar{\boldsymbol{L}}_0$ and $\bar{\boldsymbol{C}}_0$ are the longitudinal average of the zero-order PCE coefficient of the p.u.l. matrices, which in turn corresponds to their statistical average (cfr. (12a)).

With the above definitions, the Galerkin projection of (1) leads to

$$\begin{cases} \frac{d}{dz}\widetilde{\mathbf{V}}(z) = -j\omega \begin{bmatrix} \bar{\boldsymbol{L}}_0 & & \\ & \ddots & \\ & & \bar{\boldsymbol{L}}_0 \end{bmatrix} \widetilde{\mathbf{I}}(z) - j\omega\widetilde{\Delta\mathbf{L}}(z)\widetilde{\mathbf{I}}(z) \\ \frac{d}{dz}\widetilde{\mathbf{I}}(z) = -j\omega \begin{bmatrix} \bar{\boldsymbol{C}}_0 & & \\ & \ddots & \\ & & \bar{\boldsymbol{C}}_0 \end{bmatrix} \widetilde{\mathbf{V}}(z) - j\omega\widetilde{\Delta\mathbf{C}}(z)\widetilde{\mathbf{V}}(z) \end{cases} \tag{16}$$

where the diagonal matrices in the r.h.s. stem from the Galerkin projection of the deterministic components, whereas the augmented perturbation matrices $\widetilde{\Delta\mathbf{L}}$ and $\widetilde{\Delta\mathbf{C}}$ have the same structure as $\widetilde{\mathbf{L}}$ and $\widetilde{\mathbf{C}}$ in (11), yet they no longer contain the (typically dominant) average contributions.

Assuming again that the perturbation matrices are relatively small, the above equation (16) can be solved as a perturbation problem, in analogy with (4). However, thanks to the block-diagonal structure of the involved p.u.l. matrices, at every iteration the equation for each PCE coefficient can be solved independently as

$$\begin{cases} \dfrac{d}{dz}\mathbf{V}_{k,m}(z) = -j\omega\bar{\boldsymbol{L}}_0\boldsymbol{I}_{k,m}(z) + \boldsymbol{V}_{F,k,m}(z) \\ \dfrac{d}{dz}\mathbf{I}_{k,m}(z) = -j\omega\bar{\boldsymbol{C}}_0\boldsymbol{V}_{k,m}(z) + \boldsymbol{I}_{F,k,m}(z) \end{cases} \tag{17}$$

for $k = 0, \ldots, K-1$, and with

$$\begin{cases} \boldsymbol{V}_{F,k,m}(z) = & \left[-j\omega\widetilde{\Delta\mathbf{L}}(z)\widetilde{\mathbf{I}}_{m-1}(z)\right]_{\text{rows }(k-1)N+1\text{ to }kN} \\ \boldsymbol{I}_{F,k,m}(z) = & \left[-j\omega\widetilde{\Delta\mathbf{C}}(z)\widetilde{\mathbf{V}}_{m-1}(z)\right]_{\text{rows }(k-1)N+1\text{ to }kN} \end{cases} \tag{18}$$

In (17), $\boldsymbol{V}_{k,m}$ and $\boldsymbol{I}_{k,m}$ denote the approximation of the kth voltage and current PCE coefficients after m iterations, and the actual coefficients are obtained as the limit for increasing iterations, as in (7).

Thus, the proposed approach allows again the perturbative solution of the augmented MTL problem as a uniform line with distributed sources. However, the sources now simultaneously account for both variability and nonuniformity, and the solution can be carried out in a decoupled manner. At every iteration step, the very same uniform MTL with p.u.l. matrices $\bar{\boldsymbol{L}}_0$ and $\bar{\boldsymbol{C}}_0$, of size $N \times N$, is analyzed, though each time with different distributed sources. Such an MTL has the same size as the original stochastic problem. Note that this procedure resembles Jacobi's iterative method for the solution of large linear systems [24]. It is important to remark that setting a relative convergence criterion (as also described in Section II) ensures the solution preserves the high accuracy of the SGM.

V. Cost and Efficiency

The solution of an MTL equation involves the eigenvalue decomposition of the product of the p.u.l. matrices [3] or, alternatively, the calculation of their exponential stamp [20]. The cost of these operations scales superlinearly with the problem size. In the UCS method, this process is repeated for every frequency point *and* for every section, and tens to hundreds of sections are typically necessary to achieve satisfactory accuracy, depending on the electrical length and on the amount of nonuniformity [7]. On the other hand, the PT solves iteratively the same uniform line, thus requiring a single eigenvalue decomposition for each frequency point.

In order to quantify the magnitude of the perturbation matrices w.r.t. the average matrices, the following ratios are defined:

$$\begin{cases} r_L(z) = \|\widetilde{\Delta\mathbf{L}}(z)\| \;/\; \|\bar{\boldsymbol{L}}\| \\ r_C(z) = \|\widetilde{\Delta\mathbf{C}}(z)\| \;/\; \|\bar{\boldsymbol{C}}\| \end{cases} \tag{19}$$

where $\bar{\boldsymbol{L}}$ and $\bar{\boldsymbol{C}}$ take a different meaning for the two proposed methods. Namely, for the coupled implementation, they denote the average over z of the SGM-augmented matrices in (11). Instead, for the decoupled method, they denote the block-diagonal matrices in (17). Note that the 2-norm is invariant to block-diagonal repetition, thus $\|\bar{\boldsymbol{L}}\| \equiv \|\bar{\boldsymbol{L}}_0\|$ and $\|\bar{\boldsymbol{C}}\| \equiv \|\bar{\boldsymbol{C}}_0\|$ in that case.

As shown later, the number of iterations required to achieve convergence increases with the above ratios, and in general also with frequency [9]. Nonetheless, it is generally much lower than the number of sections required by the UCS method. Therefore, the standard PT can speed-up the analysis of a nonuniform MTL, and hence also MC simulations, in spite of the additional integrations required to account for the distributed sources [7].

In the first proposed method of Section III, the PT is applied as is (see Section II) to the solution of the augmented SGM equation. A uniform MTL problem of size NK with distributed sources is solved for each iteration. Alternatively, the decoupled method of Section IV solves K MTL problems of size N. Therefore, in this second case the computational cost scales roughly linearly with K, besides some overhead due to the update of the distributed sources that is common to both implementations.

For the aforementioned reasons, the proposed perturbative methods outperform the classical SGM when the number of random parameters increases. Moreover, the decoupled implementation is expected to asymptotically provide an even larger speed-up. This is illustrated in the next section.

VI. Application Examples

A. Structures Under Analysis

To investigate prediction accuracy and computational efficiency of the proposed techniques, different interconnects, characterized by an increasing number of RVs, are considered. The basic structure is depicted in Fig. 1(a). It consists of two (nominally parallel) microstrip traces printed on top of a double-sided printed circuit board (PCB). The two copper traces have length $L = 50$ mm, and thickness $t = 35$ μm. The dielectric substrate has thickness $h = 1.425$ mm, relative permittivity $\varepsilon_r = 4.4$, and loss tangent $\tan\delta = 0.001$. Ideal excitations and loads for differential signaling are considered as terminations (see Fig.1(b), where $Z_D = 100\ \Omega$ and $V_S = 1$ V). This choice mimics the loading conditions enforced by a four-port vector network analyzer (VNA) when characterizing the differential line (DL) under analysis in terms of mixed-mode S-parameters [25].

Ideally, the two traces have equal width, of nominal value $\bar{w}_1 = \bar{w}_2 = \bar{w} = 0.6$ mm, and are separated by a nominal (center-to-center) distance $\bar{D} = 1.1$ mm. However, in order to account for possible variability introduced by the manufacturing process, a random perturbation of the above parameters is introduced as detailed in the following. First, the trace widths w_1 and w_2 at either end of the DL are assumed to vary randomly around their nominal value. Accordingly, they

TABLE I
CASE STUDIES WITH NUMBER OF RVS, SGM-PROBLEM SIZE, AND MAXIMA OF PERTURBATION RATIOS r_L AND r_C OVER z-AXIS AND FREQUENCY.

Configuration		Number of signal traces N	Number of RVs d	SGM-problem size NK	$\max_{z,\omega}\{r_L\}$		$\max_{z,\omega}\{r_C\}$	
					coupled	decoupled	coupled	decoupled
1 DL	Case 1	2	4	30	0.033	0.049	0.056	0.085
	Case 2		5	42	0.032	0.069	0.052	0.161
2 DLs	Case 1	4	8	180	0.027	0.038	0.055	0.077
	Case 2		11	312	0.026	0.057	0.052	0.141
3 DLs	Case 1	6	12	546	0.025	0.034	0.055	0.077
	Case 2		17	1026	0.024	0.054	0.052	0.140
4 DLs	Case 1	8	16	1224	0.023	0.032	0.055	0.077
	Case 2		23	2400	0.022	0.055	0.053	0.140

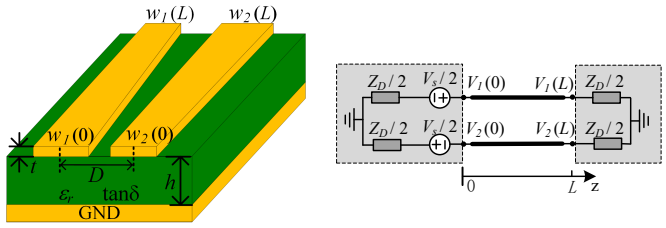

(a) (b)

Fig. 1. Differential microstrip line under analysis: (a) 3D view; (b) circuit network with terminations.

are treated as RVs normally distributed around $\bar{w}$ with a 10% relative standard deviation, i.e.,

$$\mathbf{w} = \bar{w} + 0.1 \cdot \bar{w} \cdot \boldsymbol{\xi} \tag{20}$$

where vector $\mathbf{w} = [w_1(0), w_2(0), w_1(L), w_2(L)]$ collects the trace widths at the near ($z = 0$) and far ($z = L$) end of the DL, whereas $\boldsymbol{\xi} = [\xi_1, \xi_2, \xi_3, \xi_4]$ is a set of mutually independent standard normal RVs. For each sample, the actual trace layout is obtained by connecting these random starting- and end-points, so that the traces result to be of trapezoidal shape (hence nonuniform) along the length, as shown in Fig. 1(a). This leads to the first case study in Table I, characterized by $N = 2$ signal conductors and $d = 4$ independent RVs.

The second test case is obtained by letting also the trace separation D vary randomly around $\bar{D}$ with 10% relative standard deviation, thus introducing a fifth standard normal RV, ξ_5. Further configurations, listed in Table I, are obtained by progressively including additional DLs on the same dielectric substrate, in close proximity to each other.

The last and most complex configuration, which comprises four DLs, is depicted in Fig. 2. The nominal center-to-center separation $\bar{S}$ between two adjacent traces of different pairs is twice the distance between traces belonging to the same pair, i.e., $\bar{S} = 2\bar{D}$. Like in the case of a single DL, two scenarios are considered, one with variability on the trace widths only, and one with variability in both the widths and separations. Separation variability is also considered to be normally distributed with 10% relative standard deviation. This allows generating several configurations with different problem size, in terms of both number of conductors (up to $N = 8$) and random space dimensionality (up to $d = 23$ RVs). For each test case indicated in Table I, a second-order PCE ($p = 2$) is considered, leading to a minimum number of $K = 15$ coefficients for the scenario with 4 RVs, up to $K = 300$ for the scenario with many, i.e., 23 RVs. The corresponding augmented SGM problems are of size $NK = 30$ and $NK = 2400$, respectively.

As the nominal edge-to-edge separation between trace pairs within the same DL is 0.5 mm, the lines can be considered to be tightly coupled. Anyhow, the performance of the proposed techniques is expected to be mainly influenced by the amount of variability and nonuniformity – which is expressed by the perturbation ratios (19) – rather than by coupling. The maxima of r_L and r_C over the longitudinal position z and the considered frequency range (10 MHz to 10 GHz) are also provided in Table I. It is interesting to note that these ratios are always well below unity, despite the relatively-large parameter variability. For the coupled method, similar values are observed for each test case. For the decoupled method instead, the ratios are mainly dependent on the case (i.e., on whether the trace separation is also varying or not) rather than on the overall number of RVs. Moreover, they are larger because the corresponding perturbation matrices simultaneously account for both variability and nonuniformity.

B. Numerical Results

The techniques discussed in Sections II–IV are exploited to derive statistical estimates (i.e., mean value, standard deviation, and PDFs) of the mixed-mode S-parameters of the DL structures described in the previous section. Specifically, several combinations are available, in which variability is dealt with using either MC or the SGM, and nonuniformity is tackled by means of either the UCS method or the PT. For the sake of brevity, all these techniques are hereafter denoted by aggregating the corresponding abbreviations, leading to "MC-UCS", "MC-PT", "SGM-UCS", and "SGM-PT". It should be noted that the novel SGM-PT comes in two different flavors: a fully coupled one, i.e., the method outlined in Section II, and a decoupled one, outlined in Section IV. A converge analysis showed that usually at least 10000 samples are necessary to achieve comparable accuracy between the reference MC method and the proposed SGM-PT, depending on the frequency and the specific test case. Therefore, this

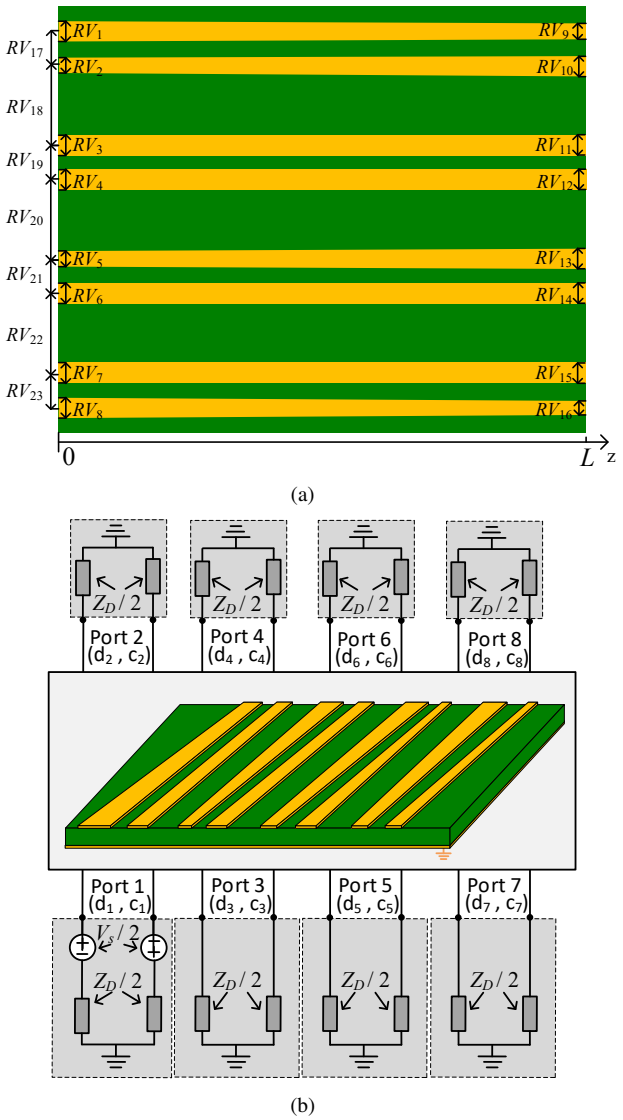

Fig. 2. Configuration with four DLs: (a) top view of one sample with 23 RVs; (b) circuit network with terminal sections. The structure is considered as a system of eight fully coupled lines.

number of runs is hereafter used as a reasonable trade-off for MC-based simulations.

For a more efficient evaluation of the frequency- and place-dependent p.u.l. matrices, as needed in all simulations, a frequency-dependent parameterized macromodel is created as a function of those parameters that vary longitudinally, i.e., the trace widths and separations (when applicable) [6]. The macromodel is constructed using data computed by means of a 2D field solver and is used to obtain samples of the p.u.l. matrices at 101 longitudinal positions. It should be noted that this approach is especially beneficial for the MC analysis, which would otherwise become prohibitive if the p.u.l. matrices had to be evaluated at each position and for each sample using the computationally expensive field solver. Specific information on the related computational times is provided in Section VI-C.

An example of the results obtained for the simplest test case (i.e., the single DL with variable trace widths) is shown in Fig. 3(a). Predictions of the mean value and standard deviation

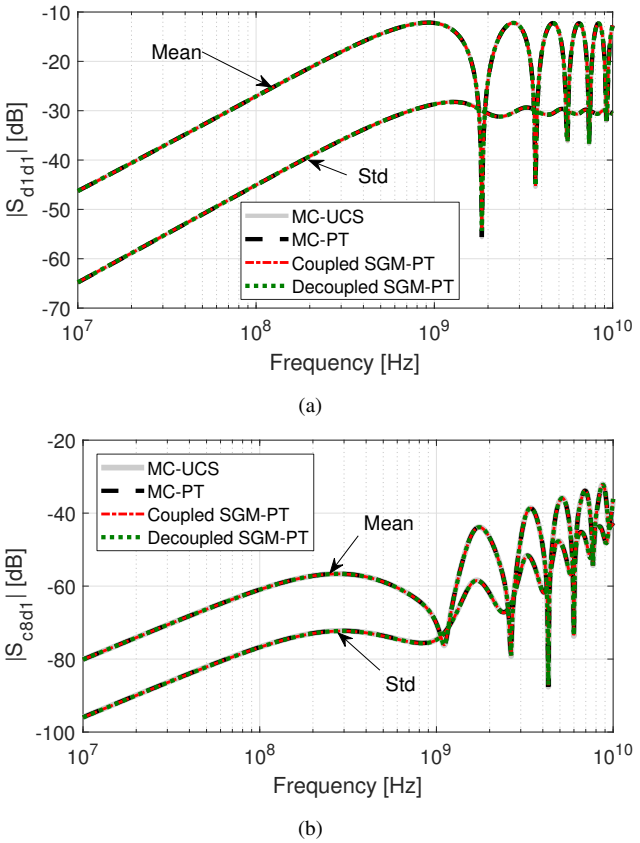

Fig. 3. Statistical estimates (average and standard deviation) of: (a) $|S_{d1d1}|$ for the single-DL structure in Fig. 1 (case 1, $N = 2$, $d = 4$); (b) $|S_{c8d1}|$ for the four-DL structure in Fig. 2 (case 2, $N = 8$, $d = 23$). Results from MC simulations (solid gray and dashed black lines) are compared against the proposed SGM-based techniques (dashed red and green lines).

of the magnitude of the S-parameter S_{d1d1} are computed at 500 frequency points in the interval from 10 MHz to 10 GHz. The plots compare the results obtained by means of four methods, establishing an excellent agreement and validating the prediction accuracy of the proposed hybrid SGM-PT strategies. This is confirmed also for the other S-parameters, although not shown here.

The case study involving 23 RVs (i.e., the sixteen-port network of Fig. 2) is considered next. The prediction accuracy is assessed in Fig. 3(b) and Fig. 4. The latter shows PDFs of $|S_{c8d1}|$ computed at two different frequencies. To calculate the SGM-PT results, 10^6 samples are extracted from the corresponding PCE. The goodness of fit of the obtained distributions is confirmed by Kolmogorov-Smirnov tests (with 5% significance level), thus demonstrating that a second-order PCE is accurate enough to reproduce the stochastic behavior of the analyzed quantities.

The number of iterations required by the coupled and de-coupled SGM-PT for two of the scenarios in Table I is plotted in Fig. 5 over frequency. It is noted that the decoupled SGM-PT requires more iterations than the coupled implementation. This is consistent with the fact that, in the former case, the perturbation ratios (19) are larger (cfr. Table I) because the distributed sources account not only for nonuniformity, but also for variability, as already noted. Nevertheless, the accuracy is not compromised, as long as a sufficient number

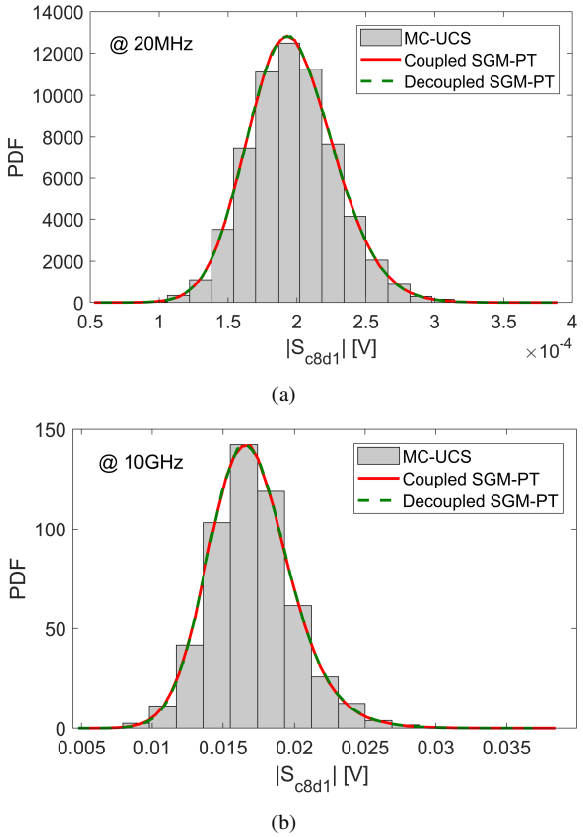

Fig. 4. PDF of $|S_{c8d1}|$ at (a) 20 MHz and (b) 10 GHz for the four-DL structure in Fig. 2 (case 2, $N = 8$, $d = 23$). Gray bars: MC-UCS; solid red line: fully coupled SGM-PT; dashed green line: decoupled SGM-PT.

of iterations is allowed in order to reach the convergence criterion. The efficiency is also improved for large problems, as discussed in the next section. Similar results are also obtained for the other test cases, which are however omitted for the sake of brevity. In all the considered test cases and frequency ranges, the iterations are always convergent, although as yet no rigorous proof could be found that guarantees convergence in general.

C. Computational Efficiency

Table II collects the computational times required for each scenario, split into three different phases. For the first test case, the MC-UCS and MC-PT simulations take 29793 s and 4329 s, respectively. The latter achieves a significant speed-up of nearly 7 times. Since similar results are obtained for the other scenarios, the former method is neglected in the following considerations, and the MC-PT is considered as the reference for computational times. The macromodel of the p.u.l. matrices is exploited by each method, hence the corresponding time is common to all techniques. The setup time refers to the generation of the random samples of the p.u.l. matrices for the MC analysis, and to the generation of the pertinent augmented matrices for the SGM-based methods. The augmented matrices for the SGM-UCS and coupled SGM-PT are the same, they are just handled differently in the simulation phase. Finally, the simulation time refers exclusively to the solution of the transmission-line equations.

TABLE II
SUMMARY OF THE COMPUTATIONAL TIMES FOR EACH TECHNIQUE.

Configuration		Method	Macromodel	Setup	Simulation
1 DL	Case 1	MC-PT	4.5 s	8.7 s	4329 s
		SGM-UCS		0.6 s	57.8 s
		Coupled SGM-PT			7.5 s
		Decoupled SGM-PT		0.6 s	10.6 s
	Case 2	MC-PT	7.5 s	15.1 s	4225 s
		SGM-UCS		0.8 s	106 s
		Coupled SGM-PT			11.4 s
		Decoupled SGM-PT		0.8 s	19.8 s
2 DLs	Case 1	MC-PT	15.0 s	26.4 s	7324 s
		SGM-UCS		1.7 s	2026 s
		Coupled SGM-PT			82.0 s
		Decoupled SGM-PT		1.7 s	77.4 s
	Case 2	MC-PT	34.9 s	85.6 s	6632 s
		SGM-UCS		3.8 s	8758 s
		Coupled SGM-PT			221 s
		Decoupled SGM-PT		3.7 s	171 s
3 DLs	Case 1	MC-PT	39.4 s	64.5 s	10038 s
		SGM-UCS		7.1 s	36556 s
		Coupled SGM-PT			888 s
		Decoupled SGM-PT		6.6 s	467 s
	Case 2	MC-PT	91.1 s	283 s	10001 s
		SGM-UCS		22.3 s	214500 s
		Coupled SGM-PT			3528 s
		Decoupled SGM-PT		22.3 s	1674 s
4 DLs	Case 1	MC-PT	90.5 s	158 s	12775 s
		SGM-UCS		23.6 s	228000 s
		Coupled SGM-PT			6017 s
		Decoupled SGM-PT		23.5 s	2270 s
	Case 2	MC-PT	222 s	607 s	12157 s
		SGM-UCS		86.0 s	1162750 s
		Coupled SGM-PT			28117 s
		Decoupled SGM-PT		94.3 s	7478 s

For a clearer picture, Fig. 6 illustrates the speed-up achieved by the various SGM implementations discussed in this paper, for all scenarios in Table I. Specifically, for the first scenario the fully coupled and decoupled SGM-PT simulations take only 12.6 s and 15.7 s in total, respectively, whereas the SGM-UCS requires 62.9 s. Hence, although the decoupled SGM-PT results to be slightly slower than the coupled implementation in this case, both methods are significantly faster than MC simulations (about 300 times) as well as than the SGM-UCS (about 5 times). For the last and most complex scenario instead, the MC-PT analysis costs 12986 s, whereas the SGM-PT simulations take 28425 s (fully coupled implementation) and 7794 s (decoupled implementation). While the coupled SGM-PT becomes approximately twice slower than the MC-PT, the proposed decoupled method still yields a significant reduction of computational time (-40%), in spite of the very large number of RVs involved.

In general, it is possible to draw the following conclusions. First of all, even in conjunction with the UCS method, the SGM is more efficient than MC-PT up to about 10 RVs. On the other hand, solving the SGM problem with the PT is always beneficial. In particular, the coupled SGM-PT implementation remains more efficient than MC up to about 20 RVs. The de-

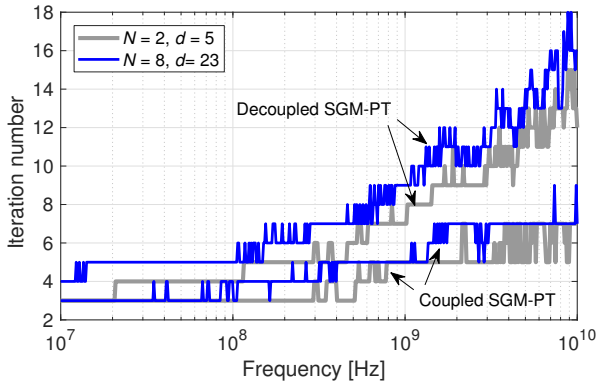

Fig. 5. Number of iterations required by the proposed perturbative methods for the test cases with $N = 2$, $d = 5$ (gray lines) and $N = 8$, $d = 23$ (blue lines).

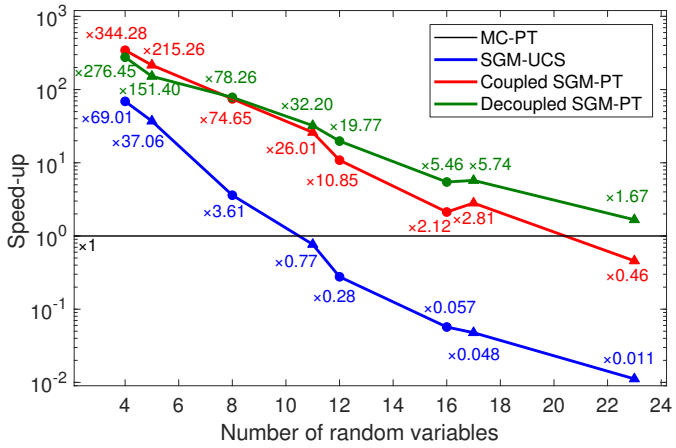

Fig. 6. Speed-up of the various SGM techniques w.r.t. the MC-PT analysis. Markers ● and ▲ refer to cases 1 and 2 in Table I, respectively.

coupled implementation allows to further extend the efficiency of the SGM beyond 23 RVs, which is an unprecedented result with the SGM. In particular, the trend of the green curve in Fig. 6 suggests that the decoupled perturbative SGM remains competitive with MC up to about 25 RVs.

It is also important to remark that the decoupled SGM-PT is slightly less efficient than the coupled one for small numbers of RVs (less than eight, in the considered test cases). This is consistent with its higher requirement in terms of iterations, as shown in Fig. 5. Beyond 8 RVs however, the impact of the SGM-problem size becomes the dominant limitation, and the benefit of decoupling prevails over the larger number of required iterations, thus making the decoupled SGM-PT performing better for problems with many RVs.

In passing, a lack of monotonicity is observed in the SGM-PT curves. This is explained by the fact that, when moving from the case with 16 RVs and 4 DLs to the one with 17 RVs and 3 DLs, the problem size actually decreases, from $NK = 1224$ to $NK = 1026$ (see Table I). This in turn reduces the computational time of all SGM-based methods. However, the SGM-UCS curve still exhibits a monotonic trend since the cost reduction is lower than in the corresponding reference MC simulation, owing to the fact that the UCS method is less efficient than the PT.

VII. Conclusions

In this paper, a hybrid perturbative-SGM method was proposed, aimed at speeding up the statistical analysis of nonuniform MTLs with geometrical/electrical parameters affected by uncertainty.

The first implementation foresees the solution of the augmented MTL problem, stemming from the application of the SGM to the original stochastic MTL under analysis, via the PT introduced in [7]. As a first step, the zero-order solution is obtained by solving an equivalent uniform line with p.u.l. matrices obtained by averaging the place-dependent p.u.l. matrices of the nonuniform augmented MTL. Line nonuniformity is then included through distributed sources, which are accounted for by iterating and updating the solutions. This method is shown to outperform traditional solution approaches based on the line subdivision into uniform cascaded sections (UCS method).

Second, a *decoupled* implementation was proposed. In this hybrid approach, new distributed sources simultaneously account for nonuniformity and variability of the p.u.l. matrices. The solution is obtained by the iterative analysis of a smaller MTL problem, having the same size as the original stochastic problem, thus achieving a better scaling and extending the efficiency to even larger random spaces.

Depending on the stopping criteria, set by the user, the proposed iterative implementations retain the desired high accuracy of the classical SGM, while allowing for faster computations. Indeed, the performance was assessed based on multiple MTL configurations with an increasing number of RVs, showing that the proposed decoupled perturbative method extends the applicability of the SGM to problems with a few tens of RVs, without compromising the accuracy. This is an unprecedented result for state-of-the-art SGM implementations.

References

[1] T. Mikazuki and N. Matsui, "Statistical design techniques for high-speed circuit boards with correlated structure distributions," *IEEE Trans. Compon. Packag. Manuf. Technol. A*, vol. 17, no. 1, pp. 159–165, Mar. 1994.

[2] J.-F. Mao and Z.-F. Li, "Analysis of the time response of nonuniform multiconductor transmission lines with a method of equivalent cascaded network chain," *IEEE Trans. Microw. Theory Techn.*, vol. 40, no. 5, pp. 948–954, May 1992.

[3] C. R. Paul, *Analysis of Multiconductor Transmission Lines*, New York: Wiley, 1994.

[4] M. Khalaj-Amirhosseini, "Analysis of nonuniform transmission lines using the equivalent sources," *Progress in Electromagnetics Research*, vol. 71, pp. 95–107, 2007.

[5] M. Chernobryvko, D. De Zutter, and D. Vande Ginste, "Nonuniform multiconductor transmission line analysis by a two-step perturbation technique," *IEEE Trans. Compon. Packag. Manuf. Techol.*, vol. 4, no. 11, pp. 1838–1846 , Nov. 2014.

[6] P. Manfredi, D. Vande Ginste, and D. De Zutter, "An effective modeling framework for the analysis of interconnects subject to line-edge roughness," *IEEE Microw. Wireless Compon. Lett.*, vol. 25, no. 8, pp. 502–504, Aug. 2015.

[7] P. Manfredi, D. De Zutter, and D. Vande Ginste, "Analysis of nonuniform transmission lines with an iterative and adaptive perturbation technique," *IEEE Trans. Electromagn. Compat.*, vol. 58, no. 3, pp. 859–867, Jun. 2016.

[8] F. Grassi, Y. Yang, X. Wu, G. Spadacini, and S. A. Pignari, "On mode conversion in geometrically unbalanced differential lines and its analogy with crosstalk," *IEEE Trans. Electromagn. Compat.*, vol. 57, no. 2, pp. 283–291, Apr. 2015.

[9] X. Wu, F. Grassi, P. Manfredi, and D. Vande Ginste, "Perturbative analysis of differential-to-common mode conversion in asymmetric nonuniform interconnects," *IEEE Trans. Electromagn. Compat.*, vol. 60, no. 1, pp. 7–15, Feb. 2018.

[10] X. Wu, F. Grassi, P. Manfredi, G. Spadacini, D. Vande Ginste, and S. A. Pignari, "Fast and accurate statistical estimation of common mode voltages and currents in weakly non-uniform differential interconnects," in *Proc. 2017 XXXII General Assembly and Scientific Symposium of the International Union of Radio Science*, Montreal, QC, Canada, Aug. 2017, pp. 1-4.

[11] D. Xiu and G. E. Karniadakis, "The Wiener-Askey polynomial chaos for stochastic differential equations," *SIAM J. Sci. Computation*, vol. 24, no. 2, pp. 619-622, 2002.

[12] P. Manfredi, D. Vande Ginste, D. De Zutter, and F. G. Canavero, "Uncertainty assessment of lossy and dispersive lines in SPICE-type environments," *IEEE Trans. Compon. Packag. Manuf. Techol.*, vol. 3, no. 7, pp. 1252–1258, Jul. 2013.

[13] A. Biondi, D. Vande Ginste, D. De Zutter, P. Manfredi, and F. G. Canavero, "Variability analysis of interconnects terminated by general nonlinear loads," *IEEE Trans. Compon. Packag. Manuf. Techol.*, vol. 3, no. 7, pp. 1244–1251, Jul. 2013.

[14] M. R. Rufuie, E. Gad, M. Nakhla, and R. Achar, "Generalized Hermite polynomial chaos for variability analysis of macro models embedded in nonlinear circuits," *IEEE Trans. Compon. Packag. Manuf. Technol.*, vol. 4, no. 4, pp. 673–684, Apr. 2014.

[15] D. Spina, F. Ferranti, G. Antonini, T. Dhaene, and L. Knockaert, "Efficient variability analysis of electromagnetic systems via polynomial chaos and model order reduction," *IEEE Trans. Compon. Packag. Manuf. Technol.*, vol. 4, no. 6, pp. 1038–1051, Jun. 2014.

[16] M. Ahadi and S. Roy, "Sparse linear regression (SPLINER) approach for efficient multidimensional uncertainty quantification of high-speed circuits," *IEEE Trans. Comput.-Aided Des. Integr. Circuits Syst.*, vol. 35, no. 10, pp. 1640–1652, Oct. 2016.

[17] P. Manfredi, D. Vande Ginste, I. S. Stievano, D. De Zutter, and F. G. Canavero, "Stochastic transmission line analysis via polynomial chaos methods: an overview," *IEEE Electromagn. Compat. Mag.*, vol. 6, no. 3, pp. 77–84, 2017.

[18] J. Bai, G. Zhang, D. Wang, A. P. Duffy and L. Wang, "Performance comparison of the SGM and the SCM in EMC Simulation," *IEEE Trans. Electromagn. Compat.*, vol. 58, no. 6, pp. 1739–1746, Dec. 2016.

[19] P. Manfredi, D. De Zutter, and D. Vande Ginste, "On the relationship between the stochastic Galerkin method and the pseudo-spectral collocation method for linear differential algebraic equations," *J. Eng. Math.*, vol. 108, no. 1, pp.73–90, Feb. 2018.

[20] R. Achar and M. S. Nakhla, "Simulation of high-speed interconnects," *Proc. IEEE*, vol. 89, no. 5, pp. 693–728, May 2001.

[21] Z. Zhang, T A. El-Moselhy, I. M. Elfadel, and L. Daniel, "Calculation of generalized polynomial-chaos basis functions and Gauss quadrature rules in hierarchical uncertainty quantification," *IEEE Trans. Comput.-Aided Des. Integr. Circuits Syst.*, vol. 33, no. 5, pp. 728–740, May 2014.

[22] C. Cui and Z. Zhang, "Stochastic collocation with non-Gaussian correlated process variations: theory, algorithms and applications," *IEEE Trans. Compon. Packag. Manuf. Techol.* (early access).

[23] P. Manfredi and F. Canavero, "Numerical calculation of polynomial chaos coefficients for stochastic per-unit-length parameters of circular conductors," *IEEE Trans. Magn.*, vol. 50, no. 3, pp. 74–82, Mar. 2014.

[24] D. M. Young, *Iterative Solution of Large Linear Systems*, Orlando: Academic Press, 1971.

[25] A. Ferrero, and M. Pirola, "Generalized mixed-mode S-parameters," *IEEE Trans. Microw. Theory Techn.*, vol. 54, no. 1, pp. 458–463, Jan. 2006.

Xinglong Wu (S'18) received the Bachelor's degree in electrical engineering (EE) from Xi'an Jiaotong University, Xi'an, China, in 2012 and the Double Master (M.Sc.) Degree in EE from Xi'an Jiaotong University and Politecnico di Milano, Milan, Italy, in 2015. He is currently working toward his Ph.D. degree in EE at Politecnico di Milano.

In March and June 2017, he was a Visiting Scientist at the Electromagnetics group, Department of Information Technology, Ghent University, Belgium. His research interests include distributed parameter circuit modeling, statistical techniques for electromagnetic compatibility (EMC), and system-level EMC.

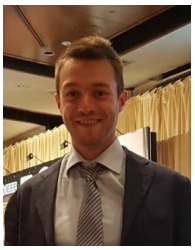

Paolo Manfredi (S'10-M'14-SM'18) received the M.Sc. degree in electronic engineering from the Politecnico di Torino, Torino, Italy, in 2009, and the Ph.D. degree in information and communication technology from the Scuola Interpolitecnica di Dottorato, Politecnico di Torino, in 2013.

From 2013 to 2014, he was a Postdoctoral Researcher with the EMC Group, Politecnico di Torino. From 2014 to 2017, he was a Postdoctoral Research Fellow of the Research Foundation–Flanders (FWO) with the Electromagnetics Group, Department of Information Technology, Ghent University, Ghent, Belgium. He is currently an Assistant Professor with the EMC Group, Department of Electronics and Telecommunications, Politecnico di Torino. His research interests comprise the several aspects of circuit and interconnect modeling and simulation, including statistical and worst-case analysis, signal integrity, and electromagnetic compatibility.

Prof. Manfredi was a recipient of an Outstanding Young Scientist Award at the 2018 Joint IEEE International Symposium on Electromagnetic Compatibility & Asia-Pacific Symposium on Electromagnetic Compatibility, the Best Paper Award at the 2016 IEEE Electrical Design of Advanced Packaging and Systems Symposium, the Best Oral Paper Award and the Best Student Paper Award at the 22nd and 19th IEEE Conference on Electrical Performance of Electronic Packaging and Systems, respectively, a Young Scientist Award at the XXX International Union of Radio Science General Assembly and Scientific Symposium, and an Honorable Mention at the 2011 IEEE Microwave Theory and Techniques Society International Microwave Symposium.

Dries Vande Ginste (SM'12) received the M.S. degree and the Ph.D. degree in electrical engineering from Ghent University, Gent, Belgium, in 2000 and 2005, respectively.

He is currently an Associate Professor at the Department of Information Technology, Ghent University and a Guest Professor at imec. In June and July 2004, he was a Visiting Scientist at the Department of Electrical and Computer Engineering, University of Illinois at Urbana-Champaign (UIUC), IL, USA. From September to November 2011, he was a Visiting Professor at the EMC Group, Dipartimento di Elettronica, Politecnico di Torino, Italy. He has authored or co-authored over 150 papers in international journals and in conference proceedings. His research interests include computational electromagnetics, electromagnetic compatibility, signal and power integrity, and antenna design.

Dr. Vande Ginste was awarded the International Union of Radio Science (URSI) Young Scientist Award at the 2011 URSI General Assembly and Scientific Symposium, the Best Poster Paper Award at the 2012 IEEE Electrical Design of Advanced Packaging and Systems Symposium (EDAPS), the Best Paper Award at the 2013 IEEE Workshop on Signal and Power Integrity (SPI), the Best Paper Award at the 2013 IEEE International Conference on Electrical Performance of Electronic Packaging and Systems (EPEPS) and the Best Paper Award at the 2016 IEEE Electrical Design of Advanced Packaging and Systems Symposium (EDAPS). He served as the chair of the 2014 IEEE Workshop on Signal and Power Integrity. He is a Senior Member of the IEEE.

Flavia Grassi (M'07-SM'13) received the Laurea (M.Sc.) and Ph.D. degrees in electrical engineering from Politecnico di Milano, Milan, Italy, in 2002 and 2006, respectively.

She is currently an Associate Professor in the Department of Electronics, Information and Bioengineering, Politecnico di Milano. From 2008 to 2009, she was with the European Space Agency (ESA), ESA/ESTEC, The Netherlands, as a Research Fellow. Her research interests include distributed-parameter circuit modeling, statistical techniques, characterization of measurement setups for EMC testing (aerospace and automotive sectors), and application of the powerline communications technology in ac and dc lines.

Dr. Grassi received the International Union of Radio Science (URSI) Young Scientist Award in 2008, and the IEEE Young Scientist Award at the 2016 Asia-Pacific International Symposium on EMC (APEMC), the IEEE EMC Society 2016 Transactions Prize Paper Award, and the Best Symposium Paper Awards from the 2015 Asia-Pacific Int. Symp. on EMC (APEMC) and the 2018 Joint IEEE EMC & APEMC Symposium.